

## EFFICIENT SCHEMES FOR REDUCING NUMERICAL DISPERSION IN MODELING MULTIPHASE TRANSPORT THROUGH POROUS AND FRACTURED MEDIA

Yu-Shu Wu<sup>1</sup> and P. A. Forsyth<sup>2</sup>

<sup>1</sup>Lawrence Berkeley National Laboratory, Berkeley, CA 94720, USA

<sup>2</sup>School of Computer Science, University of Waterloo, Waterloo, Ontario, CANADA  
e-mail: YSWu@lbl.gov

### **ABSTRACT**

Numerical issues with modeling transport of chemicals or solute in realistic large-scale subsurface systems have been a serious concern, even with the continual progress made in both simulation algorithms and computer hardware in the past few decades. The problem remains and becomes even more difficult when dealing with chemical transport in a multiphase flow system using coarse, multidimensional regular or irregular grids, because of the known effects of numerical dispersion associated with moving plume fronts. We have investigated several total-variation-diminishing (TVD) or flux-limiter schemes by implementing and testing them in the T2R3D code, one of the TOUGH2 family of codes. The objectives of this paper are (1) to investigate the possibility of applying these TVD schemes, using multi-dimensional irregular unstructured grids, and (2) to help select more accurate spatial averaging methods for simulating chemical transport given a numerical grid or spatial discretization. We present an application example to show that such TVD schemes are able to effectively reduce numerical dispersion.

### **INTRODUCTION**

Numerical approaches for modeling multiphase flow and tracer or chemical transport in porous media are generally based on methodologies developed for reservoir simulation and groundwater modeling. They involve solving coupled mass-conservation equations that govern the transport processes of all chemical components using finite-difference or finite-element schemes. Since the 1960s, in parallel with rapid advances in multiphase flow simulation and groundwater modeling, significant progress has been made in understanding and modeling solute transport through porous and fractured media (e.g., Scheidegger, 1961; Bear, 1972; Huyakorn et al. 1983; Istok, 1989; Falta et al., 1992; Unger et al. 1996; Forsyth et al. 1998; Wu and Pruess, 2000).

Since the 1970s, transport problems involving solute and contaminant migration in porous and fractured formations have received increasing attention in the groundwater literature and soil science. As demanded by site characterization, remediation, and other

environmental concerns, many quantitative modeling approaches have been developed and applied (e.g., van Genuchten and Alves, 1982; Abriola and Pinder, 1985; Corapcioglu and Baehr, 1987; Adenekan et al. 1993; Forsyth, 1994). More recently, suitability evaluation of underground geological storage of high-level radioactive wastes in unsaturated fractured rocks has generated renewed interest in investigation of tracer or radionuclide transport in a nonisothermal, multiphase fractured geological system (e.g., Viswanathan et al. 1998; Robinson et al. 2003; Moridis et al. 2003). In addition, application of tracer tests, including environmental and man-made tracers, has become an important technique in characterizing subsurface porous-medium systems.

Even with the continual progress made in both computational algorithms and computer hardware in the past few decades, modeling coupled processes of multiphase fluid flow and chemical migration in porous and fractured media remains a mathematical challenge. There still exist many unresolved issues and limitations with current numerical approaches. One of the main concerns is that severe numerical dispersion often occurs when using a multidimensional control-volume-type numerical grid in field-scale modeling studies. It becomes even more problematic when dealing with tracer transport when a general 3-D, coarse, irregular grid is used to solve advection-dispersion-type governing equations for handling tracer transport. To overcome these numerical difficulties, scientists have investigated a number of total variation diminishing (TVD) or flux limiter schemes and applied them in transport modeling with varying successes (e.g., Sweby, 1984; Liu et al. 1994; Unger et al. 1996; Forsyth et al. 1998; Oldenburg and Pruess, 1997 and 2000). However, many of these investigations were demonstrated using regular grids. This work continues the effort of reducing numerical dispersion in simulating tracer or chemical plumes as they travel spatially through porous or fractured media. The emphasis in this study is to examine the effectiveness of these TVD schemes in two- or three-dimensional, irregular, and unstructured grids.

The objectives of this paper are (1) to develop a general scheme for implementing different TVD schemes into multidimensional irregular unstructured

grids of porous or fractured media, (2) to investigate the applicability of these TVD schemes to such irregular unstructured grids, and (3) to help select more accurate spatial averaging methods for simulating chemical transport, given a numerical grid or spatial discretization.

In particular, implementation of TVD schemes is carried out using the T2R3D code, one of the TOUGH2 family of codes, made up of multidimensional, multiphase-flow, nonisothermal reservoir simulators. In this approach, a subsurface domain is discretized using an unstructured integrated-finite-difference grid, followed by time discretization carried out using a backward, first-order, finite-difference method. The final discrete linear or nonlinear equations are handled fully implicitly, using Newtonian iteration. In addition, the fractured medium is handled using a general multicontinuum modeling approach. Also, we present an application example to demonstrate that TVD schemes are in general able to reduce numerical dispersion effectively.

### **MODEL FORMULATION**

The physical processes associated with fluid flow and chemical transport in porous media are governed by fundamental conservation laws, represented mathematically (on the macroscopic level) by a set of partial differential or integral equations – governing equations. In addition, movement of dissolved mass components or chemical species within a fluid in a multiphase-porous-medium system is governed by advective, diffusive, and dispersive processes, as well as subject to other processes such as radioactive decay, adsorption, dissolution and precipitation, mass exchange or partition between phases, and other chemical reactions.

### **Governing Equation**

Let us consider a multiphase, nonisothermal system consisting of several fluid phases, such as gas, water, and oil (NAPL), with each fluid phase in turn consisting of a number of mass components. To derive a set of generalized governing equations for multiphase fluid flow, multicomponent transport, and heat transfer, we assume that these processes can be described using a continuum approach within a representative elementary volume (REV) in a porous or fractured medium (Bear, 1972). In addition, a condition of local thermodynamic equilibrium is assumed so that at any time, temperatures, phase pressures, densities, viscosities, enthalpies, internal energies, and component concentrations (or mass fractions) are the same locally at each REV of the porous medium.

According to mass and energy conservation principles, a generalized conservation equation of

mass components and energy in the porous continuum can be written as follows:

$$\frac{\partial M^k}{\partial t} = G^k + q^k + F^k \quad (1)$$

where superscript  $k$  is the index for the components,  $k = 1, 2, 3, \dots, N_c$ , with  $N_c$  being the total number of mass components and with  $k = N_c + 1$  for the energy “component” (note that thermal energy is treated as a component for convenience);  $M$  is the accumulation term of component  $k$ ;  $G^k$  is the decay or internal generation (reaction) term of mass or energy components;  $q^k$  is an external source/sink term or fracture-matrix exchange term for mass or energy component  $k$  and energy; and  $F^k$  is the “flow” term of mass or energy movement or net exchange from multiphase flow, or diffusive and dispersive mass transport, or heat transfer, as discussed below.

Under equilibrium adsorption, the accumulation term Equation (1) for component  $k$  is

$$M^k = \phi \sum_{\beta} (\rho_{\beta} S_{\beta} X_{\beta}^k) + (1 - \phi) \rho_s \rho_w X_w^k K_d^k \quad (k = 1, 2, 3, \dots, N_c) \quad (2)$$

where  $\phi$  is the porosity of porous media; subscript  $\beta$  is an index for fluid phase ( $\beta = g$  for gas,  $= w$  for aqueous phase,  $= o$  for oil);  $\rho_{\beta}$  is the density of phase  $\beta$ ; and  $S_{\beta}$  is the saturation of phase  $\beta$ ;  $X_{\beta}^k$  is the mass fraction of component  $k$  in fluid  $\beta$ ;  $\rho_s$  is the density of rock solids; and  $K_d^k$  is the distribution coefficient of component  $k$  between the aqueous phase and rock solids to account for adsorption effects. In the case in which components are subject to a first-order radioactive decay, the decay/generation term is

$$G^k = \phi \lambda_k \left( \sum_{\beta} (\rho_{\beta} S_{\beta} X_{\beta}^k) + (1 - \phi) \rho_s \rho_w X_w^k K_d^k \right) \quad (k = 1, 2, 3, \dots, N_c) \quad (3)$$

where  $\lambda_k$  is the radioactive decay constant of component  $k$ . The generation term may also be subject to other processes such as dissolution and precipitation, mass exchange and partition between phases, or chemical reactions.

The accumulation term in (1) for the heat equation is usually is defined as

$$M^{N_c+1} = \sum_{\beta} (\phi \rho_{\beta} S_{\beta} U_{\beta}) + (1 - \phi) \rho_s U_s \quad (4)$$

where  $U_{\beta}$  and  $U_s$  are the internal energies of fluid  $\beta$  and rock solids, respectively.

The mass component transport is governed in general by processes of advection, diffusion, and dispersion. Advective transport of a component or solute is carried by fluid flow, and diffusive and dispersive flux is contributed by molecular diffusion and

mechanical dispersion, or hydrodynamic dispersion. These processes are described using a modified Fick's law for the total mass flow term for a component k, by advection and dispersion, is written as

$$F^k = -\sum_{\beta} \nabla \cdot (\rho_{\beta} X_{\beta}^k \mathbf{v}_{\beta}) + \sum_{\beta} \nabla \cdot (\underline{D}_{\beta}^k \cdot \nabla (\rho_{\beta} X_{\beta}^k)) \quad (k=1, 2, 3, \dots, N_c) \quad (5)$$

where  $\mathbf{v}_{\beta}$  is a vector of the Darcy's velocity or volumetric flow, defined by Darcy's law to describe the flow of single or multiple immiscible fluids as:

$$\mathbf{v}_{\beta} = -\frac{k_{r\beta}^k}{\mu_{\beta}} (\nabla P_{\beta} - \rho_{\beta} \mathbf{g} \nabla z) \quad (6)$$

where  $P_{\beta}$ ,  $\mu_{\beta}$ , and  $\mathbf{g}$  are pressure, viscosity of fluid phase  $\beta$ , and gravitational constant, respectively;  $z$  is the vertical coordinate;  $k$  is absolute or intrinsic permeability; and  $k_{r\beta}^k$  is the relative permeability to phase  $\beta$ . In Equation (5),  $\underline{D}_{\beta}^k$  is the hydrodynamic dispersion tensor accounting for both molecular diffusion and mechanical dispersion for component  $k$  in phase  $\beta$ , defined by an extended dispersion model (Scheidegger, 1961; Bear, 1972) to include multiphase effects as

$$\underline{D}_{\beta}^k = \alpha_T^{\beta} |\mathbf{v}_{\beta}| \delta_{ij} + (\alpha_L^{\beta} - \alpha_T^{\beta}) \frac{\mathbf{v}_{\beta} \mathbf{v}_{\beta}}{|\mathbf{v}_{\beta}|} + \phi S_{\beta} \tau d_{\beta}^k \delta_{ij} \quad (k=1, 2, 3, \dots, N_c) \quad (7)$$

where  $\alpha_T^{\beta}$  and  $\alpha_L^{\beta}$  are transverse and longitudinal dispersivities, respectively, in fluid  $\beta$  of porous media;  $\tau$  is tortuosity of the porous medium;  $d_{\beta}^k$  is the molecular diffusion coefficient of component  $k$  within fluid  $\beta$ ; and  $\delta_{ij}$  is the Kronecker delta function ( $\delta_{ij} = 1$  for  $i = j$ , and  $\delta_{ij} = 0$  for  $i \neq j$ ), with  $i$  and  $j$  being coordinate indices.

Equation (5) indicates that the mass flow consists of two parts, the first part, i.e., the first term on the left-hand side, is contributed by advection in all phases, and the second part, the second term on the left-hand side of (5), is diffusive flux by hydrodynamic dispersion.

Heat transfer in porous media is in general a result of both convective and conductive processes, although in certain cases, radiation may also be involved. These heat-transfer processes are complicated by interactions between multiphase fluids, multicomponents, and associated changes in phases, internal energy, and enthalpy. Heat convection is contributed by thermal energy carried mainly by bulk flow of all fluids as well as by dispersive mass fluxes. On the other hand, heat conduction or radiation is driven by temperature gradients and may follow Fourier's law or Stefan-Boltzmann's law, respectively. Then the combined, overall heat flux term, owing to convection, conduction, and radiation in a multiphase, multicomponent, porous medium system, may be described as

$$F^{N_c+1} = -\sum_{\beta} \nabla \cdot (h_{\beta} \rho_{\beta} \mathbf{v}_{\beta}) + \sum_{\beta} \sum_k \nabla \cdot (h_{\beta}^k \underline{D}_{\beta}^k \cdot \nabla (\rho_{\beta} X_{\beta}^k)) + \nabla \cdot (\underline{K}_T \nabla T) - \varepsilon \sigma_0 T^4 \quad (8)$$

where  $h_{\beta}$  and  $h_{\beta}^k$  are specific enthalpies of fluid phase  $\beta$  and of component  $k$  in fluid  $\beta$ , respectively;  $\underline{K}_T$  is the overall thermal conductivity;  $T$  is temperature;  $\varepsilon$  is a radiation emissivity factor, and  $\sigma_0 (=5.6687 \times 10^{-8} \text{ J/m}^2 \text{ K}^4)$  is the Stefan-Boltzmann constant.

As shown in Equation (8), the total heat flow in a multiphase, multicomponent system is determined by heat convection of flow and mass dispersion [the first two terms on the right-hand side of (11)], heat conduction (the third term on the right-hand side), and thermal radiation (the last term on the right-hand side).

### Constitutive Relationships

To complete the mathematical description of multiphase flow, multicomponent transport, and heat transfer in porous media, Equation (1), a generalized mass- and energy-balance equation, needs to be supplemented with a number of constitutive equations. These constitutive correlations express interrelationships and constraints of physical processes, variables, and parameters, and allow the evaluation of secondary variables and parameters as functions of a set of primary unknowns or variables selected to make the governing equations solvable. Table 1 lists a commonly used set of constitutive relationships for describing multiphase flow, multicomponent mass transport, and heat transfer through porous media. Many of these correlations for estimating properties and interrelationships are determined by experimental studies.

### NUMERICAL FORMULATION

The methodology for using numerical approaches to simulate multiphase subsurface flow and transport consists in general of the following three steps: (1) spatial discretization of mass and energy conservation equations of Equation (1), (2) time discretization; and (3) iterative approaches to solve the resulting nonlinear, discrete algebraic equations. Among various numerical techniques for simulation studies, a mass- and energy-conserving discretization scheme, based on finite volume or integral finite-difference or finite-element methods, is the most commonly used approach, and is discussed here.

### Discrete Equations

The component mass- and energy-balance Equation (1) are discretized in space using a control-volume, integrated finite difference concept (Narasimhan and Witherspoon, 1976; Pruess, 1991). The control-

volume approach provides a general spatial discretization scheme that can represent a one-, two- or three-dimensional domain using a set of discrete meshes. Each mesh has a certain control volume for a proper averaging or interpolation of flow and transport properties or thermodynamic variables. Time discretization is carried out using a backward, first-order, fully implicit finite-difference scheme. The discrete nonlinear equations for components in the multiphase system at gridblock or node  $i$  can be written in a general form:

$$\left\{ A_i^{k,n+1} + G_i^{k,n+1} \Delta t - A_i^{k,n} \right\} \frac{V_i}{\Delta t} \quad (9)$$

$$= \sum_{j \in \eta_i} \text{flow}_{ij}^{k,n+1} + Q_i^{k,n+1}$$

( $k = 1, 2, 3, \dots, N_c, N_c+1$ ) and ( $i=1, 2, 3, \dots, N$ ) where superscript  $k$  serves also as an equation index for all mass components with  $k = 1, 2, 3, \dots, N_c$  and  $k = N_c+1$  denoting the heat equation; superscript  $n$  denotes the previous time level, with  $n+1$  the current time level to be solved; subscript  $i$  refers to the index of gridblock or node  $i$ , with  $N$  being the total number of nodes in the grid;  $\Delta t$  is time step size;  $V_i$  is the volume of node  $i$ ;  $\eta_i$  contains the set of direct neighboring nodes ( $j$ ) of node  $i$ ;  $A_i^k$ ,  $G_i^k$ ,  $\text{flow}_{ij}^k$ , and  $Q_i^k$  are the accumulation and decay/generation terms, respectively, at node  $i$ ; the “flow” term between nodes  $i$  and  $j$ , and sink/source term at node  $i$  for component  $k$  or thermal energy, respectively, are defined below.

Equation (9) has the same form regardless of the dimensionality of the system, i.e., it applies to one-, two-, or three-dimensional flow, transport, and heat-transfer analyses. The accumulation and decay/generation terms for mass components or thermal energy are evaluated using Equations (2), (3), and (4), respectively, at each node  $i$ . The “flow” terms in Equation (9) are generic and include mass fluxes by advective and dispersive processes, as described by Equation (5), as well as heat transfer, described by Equation (8). In general, the mass flow term is evaluated as (Wu and Pruess, 2000):

$$\text{flow}_{ij}^k = F_{A,ij}^k + F_{D,ij}^k \quad (k = 1, 2, 3, \dots, N_c) \quad (10)$$

where  $F_{A,ij}^k$  and  $F_{D,ij}^k$  are the net mass fluxes by advection and hydrodynamic dispersion along the connection, respectively, with

$$F_{A,ij}^k = A_{ij} \sum_{\beta} (X_{\beta}^k)_{ij+1/2} F_{\beta,ij} \quad (11)$$

where  $A_{ij}$  is the common interface area between connected blocks or nodes  $i$  and  $j$ ; and the mass flow term,  $F_{\beta,ij}$ , of fluid phase  $\beta$  is described by a discrete version of Darcy’s law, i.e., the mass flux of fluid phase  $\beta$  along the connection is given by

$$F_{\beta,ij} = \left( \frac{\rho_{\beta} k_{r\beta}}{\mu_{\beta}} \right)_{ij+1/2} \gamma_{ij} [\Psi_{\beta j} - \Psi_{\beta i}] \quad (12)$$

where  $\gamma_{ij}$  is transmissivity and is defined differently for finite-difference or finite-element discretization. If the integral finite-difference scheme (Pruess, 1991) is used, the transmissivity is calculated as

$$\gamma_{ij} = \frac{A_{ij} k_{ij+1/2}}{D_i + D_j} \quad (13)$$

where  $D_i$  is the distance from the center of block  $i$  to the interface between blocks  $i$  and  $j$ . The flow potential term in Equation (12) is defined as

$$\Psi_{\beta i} = P_{\beta i} - \rho_{\beta,ij+1/2} g Z_i \quad (14)$$

where  $Z_i$  is the depth to the center of block  $i$  from a reference datum.

For mass component transport, the flow term or the net mass flux by advection and hydrodynamic dispersion of a component along the connection of nodes  $i$  and  $j$  is determined by

$$F_{D,ij}^k = -\mathbf{n}_{ij} \cdot A_{ij} \sum_{\beta} D_{\beta}^k \cdot \nabla (\rho_{\beta} X_{\beta}^k) \quad (15)$$

where  $\mathbf{n}_{ij}$  is the unit vector along the connection of the two blocks  $i$  and  $j$ .

The total heat flux along the connection of nodes  $i$  and  $j$ , including advective, diffusive, conductive and radiation terms, may be evaluated, when using a finite-difference scheme, by

$$\text{flow}_{ij}^{N_c+1} = \sum_{\beta} \left[ (h_{\beta})_{ij+1/2} F_{\beta,ij} \right] + \sum_{\beta} \sum_k \left\{ (h_{\beta}^k)_{ij+1/2} F_{D,ij}^k \right\} + A_{ij} (K_T)_{ij+1/2} \left[ \frac{T_j - T_i}{D_i + D_j} \right] + A_{ij} \sigma_0 \epsilon_{ij+1/2} (T_j^4 - T_i^4) \quad (16)$$

In evaluating the “flow” terms in the above equations, (11)–(14), and (16), subscript  $ij+1/2$  is used to denote a proper averaging or weighting of fluid flow, component transport, or heat transfer properties at the interface or along the connection between two blocks or nodes  $i$  and  $j$ . The proper weighting of mass fraction in Equation (11) for calculating advective mass flux is the objective of this work, which is discussed in detail below. The convention for the signs of flow terms is that flow from node  $j$  into node  $i$  is defined as “+” (positive) in calculating the flow terms. Wu and Pruess (2000) present a general approach to calculating these flow terms associated with advective and dispersive mass transport and heat transfer in a multiphase system, using an irregular and unstructured multidimensional grid.

### **Spatial and Temporal Weighting and Flux Limiter Schemes**

As shown in Equations (11) and (12), there are in general two types of spatial weighting schemes needed in modeling multiphase tracer transport. The

first one,  $(X_{\beta}^k)_{ij+1/2}$ , in Equation (11) is used in estimating the averaged mass fraction for calculating advective flux, and the other  $(\rho_{\beta}k_{r\beta}/\mu_{\beta})_{ij+1/2}$  in Equation (12) is used in mobility weighting for the multiphase flow term. In the literature, flux-limiter schemes have been used not only for the first type of weighting, but also for the second type of weighting (e.g., Blunt and Rubin, 1992; and Oldenburg and Pruess, 2000). However, it has been observed in practical simulations that the numerical smearing caused by saturation fronts is in general much less severe than that with dissolved concentration fronts. Therefore, in this work, we focus our attention on the mass fraction averaging or modeling concentration plume only, whereas the traditional, full upstream weighting is used in mobility or relative permeability averaging for estimating fluid displacement or saturation fronts.

In addition to spatial weighting schemes, temporal weighting also needs to be addressed in numerical formulation. Commonly used temporal weighting schemes include fully implicit and Crank-Nicolson methods, while the fully explicit weighting is rarely used because of its strict limitation in time step size. Among these schemes, the fully implicit method has proven itself to be most effective in handling numerical problems associated with solving highly nonlinear multiphase flow equations. In particular, the theoretical analysis of advective-dispersive transport through one-dimensional finite volume grid by Unger et al. (1996) indicates that the fully implicit scheme has no limitations in Courant number under various temporal weighting schemes including flux limiters. They demonstrate how fully implicit temporal weighting leads to unconditionally stable solutions for linear advection-dispersion equation. It should be noted that fully implicit weighting is only a first-order approximation, with numerical errors of the same size as the time step. However, it is our experience (in conducting hundreds and hundreds of large, field-scale simulations of coupled multiphase flow and chemical transport) that fully implicit temporal schemes always result in stable solutions and that temporal discretization errors, caused by a fully implicit scheme, are of secondary importance in simulation, when compared with many other unknowns. The key is to have a robust numerical scheme that leads to reliable and stable solutions under different spatial discretization and various physical conditions. Considering that it is impractical to define a Peclet or Courant number for detailed theoretical analyses in most field applications when using multidimensional, irregular, unstructured grids, fully implicit temporal weighting should be selected as a first choice.

Selection of proper spatial-weighting schemes becomes very critical when dealing with coupled processes of multiphase flow, chemical transport, and heat transfer in a fractured medium. This is because fracture and matrix characteristics often greatly differ, e.g., there can be a many-orders-of-magnitude contrast in flow and transport properties, such as permeability and dispersivity. It is further complicated by the fact that there are no generally applicable weighting schemes or rules applicable to all problems or processes (Wu and Pruess, 2000). The weighting schemes that are used for flux calculation in this work are:

- Upstream weighting for relative permeability
- Harmonic or upstream weighting for absolute permeabilities for global fracture or matrix flow
- Matrix absolute permeability, thermal conductivity, molecular diffusion coefficients for fracture-matrix interaction
- Phase saturation-based weighting functions for determining diffusion coefficients
- Upstream weighted enthalpies for advective heat flow
- Central weighted scheme for thermal conductivities of global heat conduction

Consider the schematic of Figure 1, representing a multidimensional irregular, unstructured grid of porous and/or fractured media. To calculate advective flux between nodes  $i$  and  $j$ , we also need the information from a secondary upstream node (denoted as  $i2up$ ), which is an upstream node to the upstream one,  $ups(i, j)$ , between nodes  $i$  and  $j$  (Unger et al., 1996; Forsyth et al., 1998). As shown in Figure 1, the node  $i2up$  is determined by the maximum potential method in terms of maximum fluid influx into  $ups(i, j)$ . Various weighting schemes for spatially averaged mass fraction or concentration for advective flux calculation between nodes  $i$  and  $j$  are summarized as:

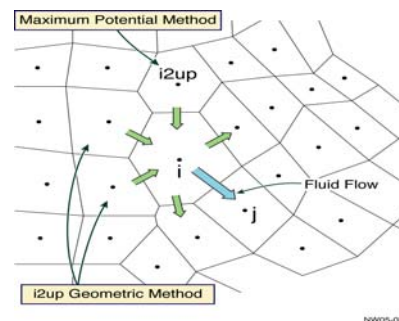


Figure 1. Schematic for determining the second upstream block ( $i2up$ ) for flow between block  $i$  and block  $j$ , using the geometric method and the maximum potential method

*Upstream:*

$$(X_{\beta}^k)_{ij+1/2} = (X_{\beta}^k)_{\text{ups}(i,j)} \quad (17)$$

where subscript ups(i, j) stands for the upstream node for fluid flow between nodes i and j.

*Central:*

$$(X_{\beta}^k)_{ij+1/2} = \frac{(X_{\beta}^k)_i + (X_{\beta}^k)_j}{2} \quad (18)$$

Several flux limiter or TVD schemes tested are as follows:

*van Leer limiter:*

$$(X_{\beta}^k)_{ij+1/2} = (X_{\beta}^k)_{\text{ups}(i,j)} + \sigma(r_{ij}) \left[ \frac{(X_{\beta}^k)_{\text{dwn}(i,j)} - (X_{\beta}^k)_{\text{ups}(i,j)}}{2} \right] \quad (19)$$

where  $(X_{\beta}^k)_{\text{dwn}(i,j)}$  is the mass fraction of downstream node of i and j, defined as

$$\text{dwn}(i, j) = i + j - \text{ups}(i, j) \quad (20)$$

The van Leer weighting factor  $\sigma(r_{ij})$  is defined as

$$\begin{aligned} \sigma(r_{ij}) &= 0 && (\text{if } r_{ij} \leq 0) \\ &= \frac{2r_{ij}}{1+r_{ij}} && (\text{if } r_{ij} > 0) \end{aligned} \quad (21)$$

with the smoothness sensor,

$$r_{ij} = \frac{\langle (X_{\beta}^k)_{\text{ups}(i,j)} - (X_{\beta}^k)_{i2\text{ups}} \rangle / (D_{\text{ups}(i,j)} + D_{i2\text{up}})}{\langle (X_{\beta}^k)_{\text{dwn}(i,j)} - (X_{\beta}^k)_{\text{ups}(i,j)} \rangle / (D_i + D_j)} \quad (22)$$

where  $D_{\text{ups}(i, j)}$  and  $D_{i2\text{up}}$  are the distances from the center of block ups(i, j) or its upstream block i2up to their common interface along the connection between the blocks.

*MUSCL Method:*

$$(X_{\beta}^k)_{ij+1/2} = (X_{\beta}^k)_{\text{ups}(i,j)} + \frac{s}{4} \left[ \left(1 - \frac{s}{3}\right) \Delta_- + \left(1 + \frac{s}{3}\right) \Delta_+ \right] \quad (23)$$

where

$$s = \frac{2\Delta_+ + \Delta_- + \varepsilon}{(\Delta_+)^2 + (\Delta_-)^2 + \varepsilon} \quad (24)$$

$$\Delta_- = \zeta \left\{ (X_{\beta}^k)_{\text{ups}(i,j)} - (X_{\beta}^k)_{i2\text{up}} \right\} \quad (25)$$

$$\Delta_+ = \left\{ (X_{\beta}^k)_{\text{ups}(i,j)} - (X_{\beta}^k)_{\text{dwn}} \right\} \quad (26)$$

and

$$\zeta = \frac{D_i + D_j}{D_{\text{ups}(i,j)} + D_{i2\text{up}}} \quad (27)$$

In (24),  $\varepsilon$  is a small number, which prevents a zero divide.

*Leonard Method:*

$$(X_{\beta}^k)_{ij+1/2} = (X_{\beta}^k)_{\text{ups}(i,j)} + \sigma(r_{ij}) \left[ \frac{(X_{\beta}^k)_{\text{dwn}(i,j)} - (X_{\beta}^k)_{\text{ups}(i,j)}}{2} \right] \quad (28)$$

where the Leonard weighting factor  $\sigma(r_{ij})$  is defined as

$$\sigma(r_{ij}) = \max \{ 0, \min(2, 2r_{ij}, (2+r_{ij})/3) \} \quad (29)$$

with  $r_{ij}$  is also defined by Equation (22).

The numerical implementation of these TVD schemes is made in the T2R3D code (Wu et al., 1996) for simulation of tracer transport through an isothermal or nonisothermal system for this work.

### Numerical Solution Scheme

There are a number of numerical solution techniques that have been developed in the literature over the past few decades to solve the nonlinear, discrete equations of flow and transport. When handling multiphase flow, multicomponent transport, and heat transfer in a multiphase flow system, investigators predominantly use a fully implicit scheme. This is because the extremely high nonlinearity inherent in those discrete equations and the many numerical schemes with different level of explicitness that may fail to converge in practice. In this section, we discuss a general procedure to solve the discrete nonlinear Equation (9) fully implicitly, using a Newton iteration method.

Let us write the discrete nonlinear Equation (9) in a residual form as

$$R_i^{k,n+1} = \left\{ A_i^{k,n+1} + G_i^{k,n+1} - A_i^{k,n} \right\} \frac{V_i}{\Delta t} \quad (30)$$

$$- \sum_{j \in \eta_i} \text{flow}_{ij}^{k,n+1} - Q_i^{k,n+1} = 0$$

$$k = 1, 2, 3, \dots, N_c + 1; \quad i = 1, 2, 3, \dots, N).$$

Equation (30) defines a set of  $(N_c+1) \times N$  coupled nonlinear equations that need to be solved for every balance equation of mass components and heat, respectively. In general,  $(N_c+1)$  primary variables per node are needed to use the Newton iteration for the associated  $(N_c+1)$  equations per node. The primary variables are usually selected among fluid pressures, fluid saturations, mass (mole) fractions of components in fluids, and temperatures. In many applications, however, primary variables cannot be fixed and must be allowed to vary dynamically to deal with phase appearance and disappearance (Forsyth et al., 1998). The rest of the dependent variables, such as relative permeability, capillary pressures, viscosity and densities, partitioning coefficients, specific enthalpies, thermal

conductivities, dispersion tensor, etc., as listed in Table 1, as well as nonselected pressures, saturations, and mass (mole) fractions, are treated as secondary variables.

In terms of the primary variables, the residual Equation (30) at a node  $i$  is regarded as a function of the primary variables at not only node  $i$ , but also at all its direct neighboring nodes  $j$ . The Newton iteration scheme gives rise to

$$\sum_m \frac{\partial R_i^{k,n+1}(x_{m,p})}{\partial x_m} (\delta x_{m,p+1}) = -R_i^{k,n+1}(x_{m,p}) \quad (31)$$

where  $x_m$  is the primary variable  $m$  with  $m = 1, 2, 3, \dots, N_c+1$ , respectively, at node  $i$  and all its direct neighbors;  $p$  is the iteration level; and  $i = 1, 2, 3, \dots, N$ . The primary variables in (31) need to be updated after each iteration:

$$x_{m,p+1} = x_{m,p} + \delta x_{m,p+1} \quad (32)$$

The Newton iteration process continues until the residuals  $R_n^{k,n+1}$  or changes in the primary variables  $\delta x_{m,p+1}$  over an iteration are reduced below preset convergence tolerances.

A numerical method is used to construct the Jacobian matrix for Equation (31), as outlined in Forsyth et al. (1995). At each Newton iteration, Equation (31) represents a system of  $(N_c+1) \times N$  linearized algebraic equations with sparse matrices, which are solved by a linear equation solver. Note that when using the flux limiter schemes, as discussed in the last subsection, advective mass flux terms in the discrete equation (21) may depend on primary and secondary variables beyond the direct neighboring nodes, such as at node of  $i2up$ . In such a situation, the Newton iteration discussed here becomes inexact, because the Jacobian matrix does not include the contributions with respect to the primary variables beyond neighboring nodes. Nevertheless, converged solutions should be correct, because the residuals are exact. This omission in these Jacobian calculations may make solution convergence more problematic. However, many numerical tests have been made for multiphase tracer transport, and no significant numerical problems have been observed.

### **Fractured Media**

The mathematical formulations and flux-limiter schemes discussed above are applicable to both single-continuum and multi-continuum media, as long as the physical processes involved can be described in a continuum sense within either continuum. When handling flow and transport through a fractured rock using the numerical formation of this section, fractured media (including explicit fracture, dual, or multiple continuum models) can be considered as special cases of unstructured grids of Figure 1. Then, a large portion of the work

consists of generating a mesh that represents both the fracture and the matrix system under consideration. Several fracture and matrix subgridding schemes exist for designing different meshes for different fracture-matrix conceptual models (e.g., Pruess, 1983).

Once a proper unstructured grid of a fracture-matrix system is generated, fracture and matrix blocks are identified to represent fracture and matrix domains, separately. Formally they are treated identically for the solution in the model. However, physically consistent fracture and matrix properties, parameter weighting schemes, and modeling conditions must be appropriately specified for both fracture and matrix systems.

### **APPLICATION**

One example is presented here to demonstrate application of the TVD schemes, as discussed above, in handling transport through fractured media. The sample problem is based on a two-dimensional site-scale model developed for investigations of the unsaturated zone at Yucca Mountain, Nevada. This example shows transport of one conservative (nonadsorbing) tracer through unsaturated fractured rock using a 2-D, unstructured grid and a dual-permeability conceptualization for handling fracture and matrix interaction.

The 2-D west-east cross-sectional model grid, shown in Figure 2, has a total of 30,000 fracture-matrix gridblocks and 74,000 connections between them in a dual-permeability mesh. The potential repository is located in the middle of the model domain, discretized with locally refined grid (Figure 2), at an elevation above 1,100 m.

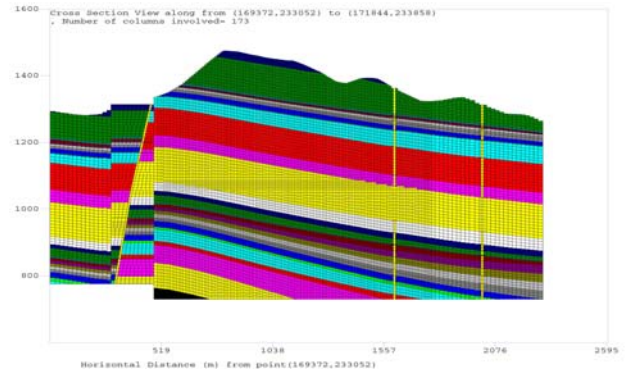


Figure 2. Two-dimensional west-east cross-sectional model domain and grid showing lateral and vertical discretization, hydrogeological layers, repository layout, and several faults incorporated

The 2-D model uses the ground surface as the top model boundary and the water table as the bottom

boundary. Both top and bottom boundaries of the model are treated as Dirichlet-type boundaries, i.e., constant (spatially distributed) pressures, liquid saturations and zero initial tracer concentrations are specified along these boundary surfaces. In addition, on the top boundary, a spatially varying, steady-state, present-day infiltration map, as shown in Figure 3, determined by the scientists of the U.S. Geological Survey, is used in this study to describe the net water recharge, with an average infiltration rate of about 5 mm/yr over the model domain. In addition, an isothermal condition is assumed in this study. The properties used for rock matrix and fractures in the dual-permeability model, including two-phase flow parameters of fractures and matrix as well as faults, were estimated from field tests and model calibration efforts (Wu et al., 2002).

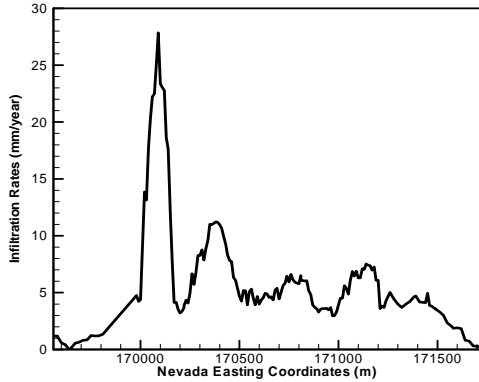


Figure 3. Net infiltration rate along the west-east cross-section model as surface water recharge boundary condition

We consider a conservative liquid tracer migrating from the repository downward by advective and dispersive processes, subject to the ambient steady-state unsaturated flow condition. A constant effective molecular diffusion coefficient of  $3.2 \times 10^{-11}$  (m<sup>2</sup>/s) is used for matrix diffusion of the conservative component. Transport starts with a finite amount of the tracer initially released into the fracture elements of the repository blocks. After the simulation starts, no more tracer will be introduced into the system, but the steady-state water recharge from the top boundary continues. Eventually, all the tracer will be flushed out from the 2-D system through the bottom, water table boundary, by advective and diffusive processes.

Figures 4 and 5 show normalized tracer concentration contours in the fracture continuum within the 2-D model at 10 years of tracer release, simulated using various weighting schemes of spatially averaged

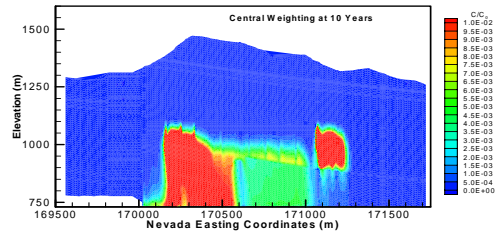


Figure 4. Concentration distributions within the 2-D model at 10 years, simulated using the central weighting scheme mass fraction for advective flux calculation.

Comparisons of simulated concentrations between Figures 4 (central weighting) and 5 (TVD-MUSCL) show a large difference at the time of 10 years. Note that for this problem, all three TVD schemes implemented in this study give similar results, so only the results with MUSCL are shown for the TVD cases in Figure 5. Figure 6 presents fractional cumulative mass breakthrough curves at the water table, also showing some significant difference between the results using the TVD schemes and the central weighting.

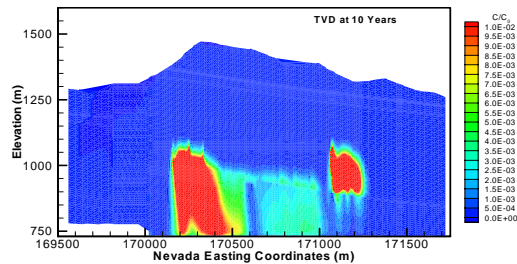


Figure 5. Concentration distributions within the 2-D model at 10 years, simulated using the TVD (MUSCL) scheme

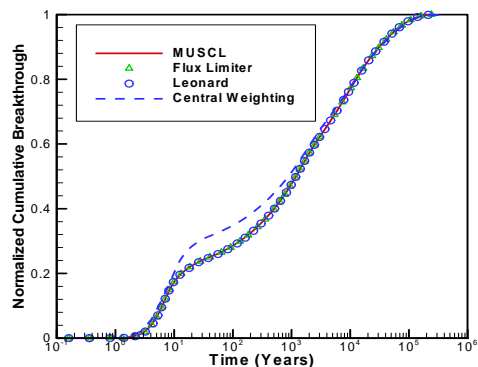


Figure 6. Breakthrough curves of fractional cumulative tracer mass arriving at the water table, since release from the repository, simulated using the different weighting schemes

Overall, the simulation results indicate that at early time, such as in first 10 years (Figure 4), the central weighting scheme underestimates advective transport, while at later time ( $t > 100$  years) it overestimates advective transport, because of selecting too high or too low averaged concentration values. In addition, the TVD schemes are tested and found to have much better numerical performance than the central weighting scheme with respect to taking larger time steps or stability.

### **SUMMARY AND CONCLUSIONS**

We have investigated several TVD schemes by implementing them into the TOUGH2 family of codes, using multidimensional irregular unstructured grids. Our test results show that such TVD schemes are able to reduce numerical dispersion effectively, if used properly. In addition, numerical performance with TVD schemes is significantly improved than commonly used central weighting and is comparable to fully upstream weighting. It is encouraging to note that under multiphase conditions using relatively coarse spatial discretization, these TVD schemes provide more accurate simulation results for modeling large-scale field tracer transport processes through heterogeneous, fractured rock.

### **ACKNOWLEDGMENTS**

The authors would like to thank Leihau Pan for his help with the model grid. Thanks are also due to Guoxiang Zhang and Dan Hawkes for their review of the paper. This work was supported in part by the U.S. Department of Energy. The support is provided to Berkeley Lab through the U. S. Department of Energy Contract No. DE-AC03-76SF00098.

### **REFERENCES**

Abriola, L. M. and G. F. Pinder, A Multiphase Approach to the Modeling of Porous Media Contamination by Organic Compounds, 1. Equation Development, *Water Resources Research*, Vol. 21, No. 1, pp. 11-18, 1985.

Adenekan, A. E., T. W. Patzek and K. Pruess, Modeling of Multiphase Transport of Multicomponent Organic Contaminants and Heat in the Subsurface: Numerical Model Formulation, *Water Resources Research*, Vol. 29, No. 11, pp. 3727-3740, 1993.

Bear, J., *Dynamics of Fluids in Porous Media*, American Elsevier Publishing Company, New York, 1972.

Blunt, M. and B. Rubin, Implicit Flux limiting Schemes for Petroleum Reservoir Simulation, *J. Comp. Phys.*, pp.194-210, 1992.

Corapcioglu, M. Y. and A. L. Baehr, A Compositional Multiphase Model for Groundwater Contamination by Petroleum Products, 1. Theoretical Considerations, *Water Resources Research*, Vol. 23, No. 1, pp. 191-200, 1987.

Falta, W. R., K. Pruess, I. Javandel and P. A. Witherspoon, Numerical Modeling of Steam Injection for the Removal of Nonaqueous Phase Liquids from the Subsurface, 1. Numerical Formulation, *Water Resources Research*, Vol. 28, No. 2, pp. 433-449, 1992.

Forsyth, P. A., A. J. A. Unger and E. A. Sudicky, Nonlinear Iteration Methods for Nonequilibrium Multiphase Subsurface Flow, *Advances in Water Resources*, Vol. 21, pp. 433-499, 1998.

Forsyth, P. A., Y. S. Wu and K. Pruess, Robust Numerical Methods for Saturated-Unsaturated Flow with Dry Initial Conditions in Heterogeneous Media, *Advances in Water Resources*, Vol. 18, pp. 25-38, 1995.

Forsyth, P. A., Three-Dimensional Modeling of Steam Flush for DNAPL Site Remediation, *International Journal for Numerical Methods in Fluids*, Vol. 19, 1055-1081, 1994.

Huyakorn, P. S., B. H. Lester and J. W. Mercer, An Efficient Finite Element Technique for Modeling Transport of Fractured Porous Media, 1. Single Species Transport, *Water Resources Research*, Vol. 19, No. 3, pp. 841-854, 1983.

Istok, J., *Groundwater Modeling by the Finite Element Method*, American Geophysical Union Water Resources Monograph 13, 1989.

Liu, J., M. Delshad, G. A. Pope, and K. Sepehrnoori, Application of higher-order flux-limited methods in compositional simulation, *Transport in Porous media*, 16, pp.1-29, 2004.

Moridis G. J., Q. Hu, Y. S. Wu, and G. S. Bodvarsson, Preliminary 3-D site-scale studies of radioactive colloid transport in the unsaturated zone at Yucca Mountain, Nevada, *Journal of Contaminant Hydrology*, 60, 251-286, 2003.

Narasimhan, T. N. and Witherspoon, P.A., An Integrated Finite Difference Method for Analyzing Fluid Flow in Porous Media, *Water Resources Research*, 12(1), pp. 57-64, 1976.

Oldenburg, C.M., and K. Pruess, Simulation of propagating fronts in geothermal reservoirs with the implicit Leonard total variation diminishing scheme, *Geothermics*, 29(2000), 1-25, 2000.

Oldenburg, C. M. and K. Pruess, Higher-Order Differencing for Geothermal Reservoir Simulation, Proceedings of Twenty-Second Workshop on Geothermal Reservoir Engineering, Stanford University, Stanford, California, January 27-29, 1997.

Pruess, K., *TOUGH2 - A General-Purpose Numerical Simulator for Multiphase Fluid and Heat Flow*, Report LBL-29400, Lawrence Berkeley National Laboratory, Berkeley, California, 1991.

Pruess, K., GMINC - A Mesh Generator for Flow Simulations in Fractured Reservoirs, Report LBL-15227, Berkeley, California: Lawrence Berkeley National Laboratory, 1983.

Robinson, B. A., C. Li, and C. K. Ho, Performance assessment model development and analysis of radionuclide transport in the unsaturated zone, Yucca Mountain, Nevada, *Journal of Contaminant Hydrology*, 62-63, 249-268, 2003.

Scheidegger, A. E., General Theory of Dispersion in Porous Media, *J. Geophys. Res.*, Vol. 66, pp. 3273-3278, 1961.

Sweby, P. K., High resolution schemes using flux limiters for hyperbolic conservation laws, *SIAM J. Num. Anal.*, 21, pp.995-1011, 1982.

Unger, A. J. A., P. A. Forsyth, and E. A. Sudicky, Variable Spatial and Temporal Weighting Schemes for Use in Multi-phase Compositional Problems, *Advances in Water Resources*, Vol. 19, No. 1, pp. 1-27, 1996.

Viswanathan, H. S., B. A. Robinson, A. J. Valocchi, A. J. and I. R. Triay, I. R. A Reactive transport model of neptunium migration from the potential repository at Yucca Mountain, *Journal of Hydrology*, 209, 251-280, 1998.

Wu, Y. S., L. Pan, W. Zhang, and G. S. Bodvarsson, Characterization of flow and transport processes within the unsaturated zone of Yucca Mountain, Nevada, *Journal of Contaminant Hydrology*, 54, 215-247, 2002.

Wu, Y.S. and K. Pruess, Numerical simulation of non-isothermal multiphase tracer transport in heterogeneous fractured porous media, *Advance in Water Resources*, 23, 699-723, 2000.

Wu, Y.S., C.F. Ahlers, P. Fraser, A. Simmons and K. Pruess, Software Qualification Of Selected TOUGH2 Modules, Report LBL-39490; UC-800, Lawrence Berkeley National Laboratory, Berkeley, CA, 1996.

Table 1. Constitutive Relationships and Functional Dependence

Definition	Function	Description
Capillary pressure	$P_{C\beta} = P_{C\beta}(S_{\beta})$	In a multiphase system, the capillary pressure relates pressures between the phases and is defined as a function of fluid saturation.
Equilibrium adsorption	$X_s^k = K_d^k \rho_{\beta} X_{\beta}^k$	$X_s^k$ is the mass of component k sorbed per mass of solids; and the distribution coefficient, $K_d^k$ , is treated as a constant or as a function of the concentration or mass fraction in a fluid phase
Equilibrium partitioning	$\omega_{\alpha}^k = K_{\alpha\beta}^k \omega_{\beta}^k$	$\omega_{\alpha}^k$ and $\omega_{\beta}^k$ are the mole fraction of component k in phase $\alpha$ and $\beta$ , respectively; and $K_{\alpha\beta}^k$ is the equilibrium partitioning coefficient of component k between phases $\alpha$ and $\beta$ .
First-order decay constant	$\lambda_k = \frac{\ln(2)}{T_{1/2}}$	$T_{1/2}$ is the half-life of the radioactive component.
Fluid density	$\rho_{\beta} = \rho_{\beta}(P, T, X_{\beta}^k)$	Density of a fluid phase is treated as a function of pressure and temperature, as well as mass compositions ( $k = 1, 2, 3, \dots, N_c$ ).
Fluid saturation	$\sum_{\beta} S_{\beta} = 1$	Constraint on summation of total fluid saturation.
Fluid viscosity	$\mu_{\beta} = \mu_{\beta}(P, T, X_{\beta}^k)$	The functional dependence or empirical expressions of viscosity of a fluid is treated as a function of pressure, temperature, and composition.
Henry's law	$P_g^k = K_H^k \omega_w^k$	$P_g^k$ is partial pressure of component k in gas phase; $K_H^k$ is Henry's constant for component k; and $\omega_w^k$ is the mole fraction of component k in water phase.
Mass fraction	$\sum_k X_{\beta}^k = 1$	Constraint on mass fractions within phase $\beta$ .
Partitioning coefficient	$K_{\alpha\beta}^k = K_{\alpha\beta}^k(P_{\beta}, T, X_{\beta}^k)$	depends on chemical properties of the component and is a function of temperature, pressure, and composition.
Porosity	$\phi = \phi^{\circ}(1 + C_r(P - P^{\circ}) - C_T(T - T^{\circ}))$	$\phi^{\circ}$ is the effective porosity at a reference pressure, $P^{\circ}$ , and a reference temperature, $T^{\circ}$ ; and $C_r$ and $C_T$ are the compressibility and thermal expansion coefficient of the medium, respectively.
Radioactive decay	$C_{\beta}^k = C_{\beta 0}^k e^{-\lambda_k t}$	$C_{\beta}^k$ is the concentration of component k in phase $\beta$ and is equal to $C_{\beta 0}^k$ at $t = 0$ ; $\lambda_k$ is the radioactive decay constant.
Relative permeability	$k_{r\beta} = k_{r\beta}(S_{\beta})$	The relative permeability of a fluid phase in a multiphase system are normally assumed to be functions of fluid saturation.
specific enthalpies of gas	$h_g^k = U_g^k + \frac{P_g^k}{C_g^k}$	$U_g^k$ the specific internal energy of component k in the gas phase; $C_g^k$ concentration of component k in gas phase ( $\text{kg}/\text{m}^3$ ).
specific enthalpy of liquid	$h_{\beta} = U_{\beta} + \frac{P_{\beta}}{\rho_{\beta}}$	Internal energy, $U_{\beta}$ , of liquid phase $\beta$ is a function of pressure and temperature.
thermal conductivity	$K_T = K_T(S_{\beta})$	The thermal conductivity of the porous medium is treated as a function of fluid saturation.